Proceedings of the Combustion Institute, Volume 29, 2002/pp. 345–351

CF_3Br AND OTHER SUPPRESSANTS: DIFFERENCES IN EFFECTS ON FLAME STRUCTURE

BRADLEY A. WILLIAMS AND JAMES W. FLEMING
Chemistry Division, Code 6185
Naval Research Laboratory
Washington, DC 20375-5342, USA

We report the results of modeling studies of premixed, atmospheric pressure, methane/air flames inhibited by the following agents: N_2, CF_4, $Fe(CO)_5$, NaOH, CF_3CHFCF_3, CF_3CH_2F, and CF_3Br. These agents comprise inert, catalytic, and hydrofluorocarbon suppressants. The effects on the flame structure and chemistry of CF_3Br, which is often used as a benchmark for alternative fire suppressants, are compared to those of the other agents. These comparisons show that the behavior of CF_3Br is atypical of fire suppressants which act by efficient catalytic scavenging of flame radicals. Chemical saturation effects, dependence of inhibition efficiency on flame temperature, and changes in flame structure all differ significantly between CF_3Br and other catalytic substances, including iron and alkali metals. Various correlations proposed between burning velocity and global flame properties such as peak radical concentrations all break down for one or more of the suppressants studied. Comparison of flame structure results show that this effect results from non-uniform reduction of radical concentrations throughout the flame; both CF_3Br and non-brominated fluorocarbons cause the greatest relative reduction of radicals early in the flame. The use of CF_3Br as a performance benchmark for new fire suppressants is appropriate from an engineering standpoint. The atypical aspects of CF_3Br's behavior compared to other chemical inhibitors, however, indicates that care is required in inferring general principles in structure and chemistry of suppressed flames.

Introduction

The production ban on CF_3Br (halon 1301) has led, paradoxically, to increased research devoted to understanding its mechanism of suppressing combustion. Implicit in these studies is the assumption that detailed knowledge of the suppression mechanism and performance of CF_3Br will prove a useful guide in identifying new classes of suppressants whose effectiveness is equal to or greater than that of CF_3Br.

Since much of the recent research on fire safety has been focused on finding environmentally acceptable alternatives to CF_3Br to provide equivalent protection against a specified fire threat, the effectiveness of the prospective substitute agent relative to CF_3Br in practical situations is an important parameter for system engineering. Additionally, the inhibition properties and flame chemistry of CF_3Br have been studied for many years [1–5], so knowledge of its behavior far exceeds that of most other suppressants. For this reason, CF_3Br has often been considered in both experimental and modeling studies as a representative suppressant.

The question remains of how applicable the knowledge gained in recent years on CF_3Br will be to identifying alternative suppressants. Is CF_3Br "typical" of efficient fire suppressants in general? Will all promising replacements for CF_3Br show similar behavior? Is commonality of properties with CF_3Br a useful guide in the search for alternatives? To this end, we have performed modeling studies of premixed flames containing substances representative of different classes of inhibitors, including inert gases, fluorocarbons, and catalytic scavengers of flame radicals. While suppression of non-premixed flames is the typical scenario in fire extinguishment, the behavior of suppression agents in premixed flames is important in mitigating deflagrations and protecting against reignition. Furthermore, a large body of suppression data in different types of flames compiled by Babushok and Tsang [2] shows that for many agents, extinction of non-premixed flames correlates with reduction of burning velocity in premixed flames.

Types of Suppressants

Suppressants may be categorized based on how they inhibit combustion [6]. We term as "physical suppressants" substances (such as nitrogen, argon, CF_4, and water) which do not participate in flame chemistry to a significant extent. Physical agents inhibit combustion principally by adding heat capacity and by diluting the reactants. By contrast, "chemical

suppressants" are substances which do participate in flame chemistry.

Chemical suppressants may be subdivided into two groups: catalytic suppressants (including bromine, iodine, and various metallic elements) reduce concentrations of flame radicals through a regenerative cycle in which one molecule of suppressant recombines several flame radicals, whereas non-catalytic chemical suppressants (e.g., fluorocarbons) reduce concentrations of flame radicals by scavenging, but do not support a catalytic cycle and are generally less effective. With the exception of water mist [7], all highly effective agents identified to date are catalytic scavengers [2]. Although CF_3Br is viewed as a catalytic suppressant due to an H + H recombination cycle involving the bromine atom, the fluorocarbon moiety contributes some non-catalytic suppression as well [6]. The bromine scavenging cycle has relatively modest efficiency compared to the cycles of a number of other elements, including alkali and transition metals [2,5].

Here we compare the effect on burning velocity and structure of CF_3Br with those of the catalytic inhibitors NaOH and $Fe(CO)_5$, the non-catalytic hydrofluorocarbons CF_3CHFCF_3 (HFC-227ea) and CF_3CH_2F (HFC-134a), and the inert agents N_2 and CF_4. CF_4 undergoes little decomposition in the reaction zone of most flames [8] and is thus a physical agent.

Computational Methodology

The PREMIX code [9] was used to compute burning velocities and flame structures of atmospheric pressure, stoichiometric methane/air flames with and without suppressants. A domain of 85 cm was used in the calculations, extending 25 cm from the reaction zone on the cold boundary and 60 cm from the reaction zone on the hot boundary. The mesh extension and refinement were so that the spacing between the outermost grid points on each boundary was 1 cm, to minimize any temperature or species gradients at the boundaries. Multicomponent transport formulations, as well as the Soret effect for the species H and H_2, were used for all calculations. Refinement tolerances of 0.1 for the normalized species gradient (GRAD keyword) and 0.2 for the normalized second derivative (CURV keyword) were used for all calculations. The final meshes typically contained 90–125 grid points, depending on the number of additional species introduced by the inhibitor chemistry.

Comparison of the PREMIX results with thermal equilibrium calculations for several inhibited and uninhibited flames showed that at the final grid point, temperatures were within 5 K and radical concentrations of H, OH, and O within a few percent of their equilibrium values. Thus, in the discussion below, the radical equilibrium values and adiabatic temperatures were assumed to be those calculated at the hot boundary. All flames were stoichiometric, atmospheric pressure methane/air, with the inhibitors listed above added in various concentrations. For the hydrocarbon chemistry, the GRI-MECH 2.11 [10] (excluding nitrogen chemistry) was used as the chemical kinetic mechanism. For the uninhibited, stoichiometric methane/air flame, a predicted burning velocity of 39.5 ± 0.2 cm/s was obtained.

The fluorocarbon chemistry was based on the mechanism developed by Westmoreland et al., as refined in previous studies performed in our laboratory [11,12]. The bromine chemistry used in the modeling of CF_3Br was that developed by Noto et al. [3]. The kinetic mechanism for NaOH was based on that of Zamansky et al. [13], while that for $Fe(CO)_5$ was described by Rumminger and Linteris [14]. NaOH must vaporize before being able to participate in the flame chemistry, but the PREMIX code has no provision for inclusion of condensed-phase species. To simulate the evaporation effect, the sodium hydroxide was therefore assumed to initially consist of the gas-phase dimer $Na_2O_2H_2$, which was required to dissociate (ΔH_f = 42 kcal/mol) before inhibition chemistry could proceed. N_2 and CF_4 were assumed inert: no nitrogen or fluorine chemistry was included in the respective calculations.

Inhibition Parameter

The effectiveness of an inhibitor at reducing burning velocity in a fuel/oxidizer mixture may be placed on a quantitative basis in terms of the inhibition parameter Φ proposed by Rosser et al. [15] and modified by Noto et al. [3]:

$$\Phi = \ln(U_0/U_i)(X_{O2}/X_i) \quad (1)$$

where U_0 and U_i are the burning velocities of the uninhibited and inhibited flames, respectively, and X_{O2} and X_i are the reactant mole fractions of oxygen and inhibitor. In Ref. [3], the burning velocity of a given fuel/air mixture was found to exhibit an exponential dependence on concentrations of several inert and fluorocarbon inhibitors, including CF_3Br. A constant value of Φ with inhibitor concentration indicates that the exponential behavior found in Ref. [3] holds.

Catalytic radical scavengers necessarily manifest saturation effects, because catalysis cannot reduce concentrations of flame radicals below the thermal equilibrium level at the local flame temperature. The existence of a similarity transform, obtained by solving Equation 1 for U_i [3], which causes the flame speed reduction curves for CF_3Br *and* noncatalytic agents to coincide, is thus somewhat unexpected.

Changes in burning velocity, adiabatic flame temperature, radical superequilibrium, and inhibition

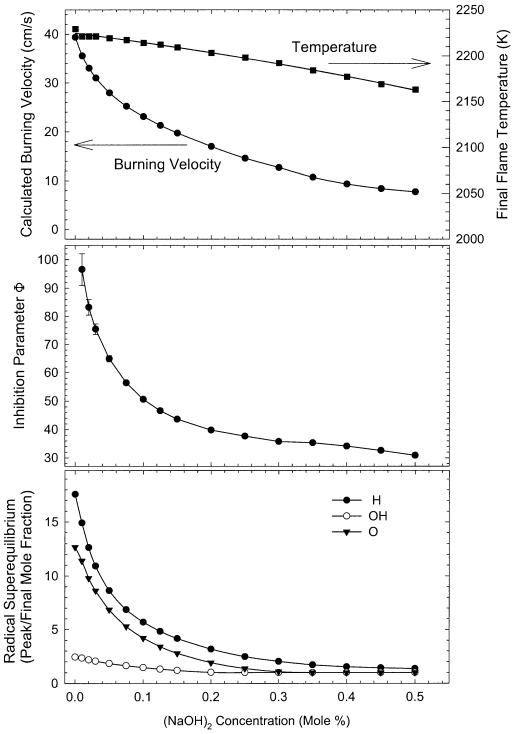

FIG 1. Burning velocity, final flame temperature, inhibition parameter (equation 1), and superequilibrium concentrations (see text) of flame radicals computed for atmospheric pressure stoichiometric methane/air mixtures inhibited by sodium hydroxide. To simulate the evaporation process, NaOH was added to the reactants as a dimer and required to undergo an endothermic decomposition process before inhibition chemistry could occur.

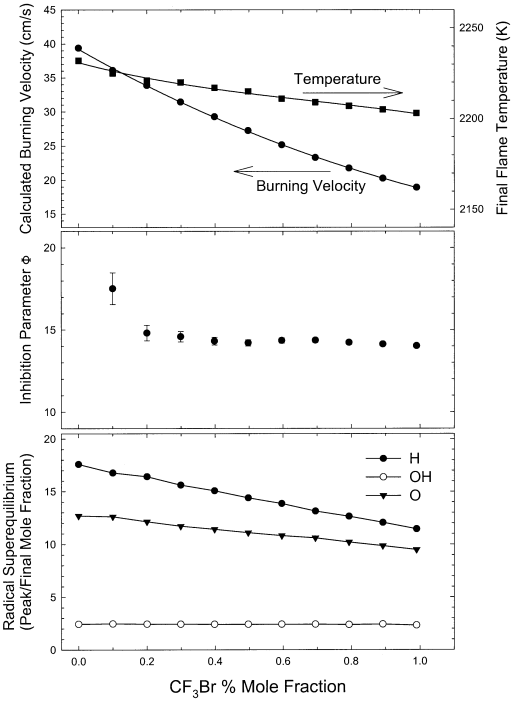

FIG 2. Burning velocity, final flame temperature, inhibition parameter (equation 1), and superequilibrium concentrations of flame radicals computed for atmospheric pressure stoichiometric methane/air mixtures inhibited by CF_3Br.

parameter Φ are plotted as a function of $(NaOH)_2$ concentration in Fig. 1 and CF_3Br concentration in Fig. 2. Error bars for Φ were determined by propagating a change of 0.2 cm/s in the inhibited flame speed (the estimated computational uncertainty for the mesh refinement tolerances used) to determine the change in Φ in equation 1; the points at low inhibitor concentrations have high uncertainties in Φ due to the small reductions in burning velocities. We define the radical superequilibrium as the ratio of the peak concentrations of the radical to its concentration at thermal equilibrium at the adiabatic flame temperature. The value for this ratio will always be unity or greater; greater than unity means the radical exists in superequilibrium concentration somewhere in the flame.

Comparing the inhibition parameter in Figs. 1 and 2, dramatically different behavior is seen. For sodium, the inhibition parameter is not constant as a function of inhibitor concentration, but varies by more than a factor of 3 over the range of sodium concentrations considered here. The similarity relationship identified in Ref. [3] does not hold for sodium. For CF_3Br, by contrast, the inhibition parameter is nearly constant as a function of inhibitor concentration. By comparison, for the inhibition parameter of N_2, up to a 50% reduction in burning velocity maintains an almost constant value of 0.5 (data not shown). The present results for CF_3Br agree with the findings of Noto et al. [3], although the modifications to the fluorocarbon kinetics yield better agreement with the experimental value of 14.0 for the inhibition parameter, compared to the value of 11.1 reported in Ref. [3]. The value of approximately 100 for the inhibition parameter of $(NaOH)_2$ per sodium atom at low concentrations compares to values obtained from experimental data on various sodium compounds ranging from 114 to 200 [2].

Radical Superequilibrium

In Fig. 1, the radical superequilibrium is drastically reduced with increasing NaOH. For inert agents, by contrast, the radical superequilibrium is increased as the flame is inhibited. When the flame

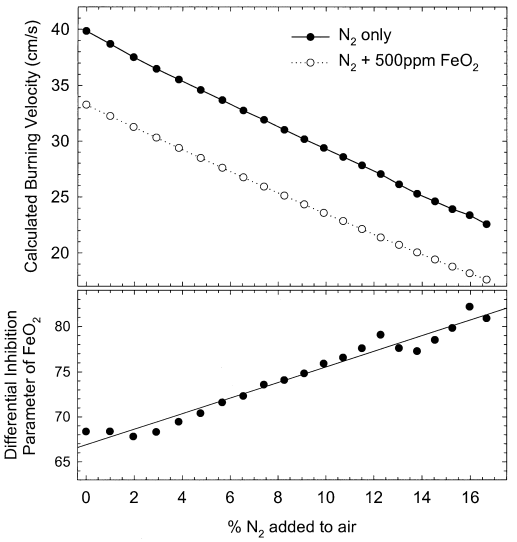

FIG 3. Burning velocity and differential inhibition parameter (equation 2) computed for atmospheric pressure stoichiometric methane/air mixtures inhibited by nitrogen and FeO_2 in combination.

speed is reduced by 40% by addition of N_2, for example, the H-atom superequilibrium increases from 17 to 70. Although peak radical concentrations decrease as an inert agent is added, the reduction in flame temperature reduces the equilibrium concentrations proportionately more.

For inhibition by CF_3Br (Fig. 2), the degree of radical superequilibrium is also reduced with increasing agent concentration, although not as dramatically as for sodium. CF_3Br reduces the H-atom superequilibrium by only 30% for a 50% reduction in burning velocity; NaOH reduces the H-atom superequilibrium by nearly 80% at a 50% burning velocity reduction. This finding supports the conclusion of Saso et al. [4] that saturation is a minor effect in the suppression effectiveness of CF_3Br/inert mixtures. Saturation is not as pronounced for CF_3Br inhibition because the peak radical concentrations remain far from equilibrium for substantial reductions in burning velocity.

Another factor contributing to the lack of a saturation behavior for CF_3Br is that the bromine catalytic cycle involves the sequence of reactions [1]

$$Br + Br + M \Rightarrow Br_2 + M \qquad (R1)$$

$$H + Br_2 \Rightarrow HBr + Br \qquad (R2)$$

as an important pathway in regeneration of HBr. The direct reaction

$$H + Br + M \Rightarrow HBr + M \qquad (R3)$$

has slow kinetics. This has two consequences: the second-order dependence of reaction R1 on the bromine concentration compensates for the saturation effect with increasing CF_3Br concentration. Also, a high concentration of bromine is required for this reaction to be significant, leading to a much smaller inhibition parameter for bromine than for iron and sodium [2], whose scavenging cycles are not thought to depend on second-order kinetics.

Synergism between Catalytic and Physical Agents

Several experimental and modeling studies have observed that the effectiveness of CF_3Br [4,16] as well as other chemical agents [17,18] can be enhanced by the addition of a physical agent. Saso et al. [4] attributed synergism in mixtures of CF_3Br and inert inhibitors to a temperature effect on the inhibition effectiveness of CF_3Br, rather than a saturation phenomenon. Over a range of adiabatic flame temperatures, Saso et al. found CF_3Br to have virtually identical inhibition parameters at concentrations of 0.5% and 1% in methane/oxygen/inert mixtures, indicating the absence of significant saturation effects.

To extend the computational investigation of synergy to other combinations of agents, inhibition by iron was modeled in combination with nitrogen. For this modeling, iron was considered to participate in a three-step mechanism involving only O + O recombination. This pathway was identified by Rumminger and Linteris [14], but is usually secondary in importance to an H + H recombination pathway. This model is *not* intended as an accurate description of iron's combustion chemistry, but rather to consider whether synergism occurs in the absence of a temperature dependence on the inhibition kinetics.

Of the three reactions making up the O + O catalytic cycle of iron:

$$Fe + O_2 + M \Rightarrow FeO_2 + M \qquad (R4)$$

$$FeO_2 + O \Rightarrow FeO + O_2 \qquad (R5)$$

$$FeO + O \Rightarrow Fe + O_2 \qquad (R6)$$

R5 and R6 are assumed to have rate coefficients independent of temperature. Reaction R4 has a slight increase in rate with increasing temperature, but the product of the rate coefficient and the number density of third-body colliders varies by less than 10% over the temperature range from 1400 and 2500 K.

The iron + nitrogen combination exhibits synergy, as seen in Fig. 3, which plots burning velocity and differential inhibition parameter of the O + O cycle of 500 ppm FeO_2 as a function of nitrogen addition. We define the differential inhibition parameter for inhibitor B in the presence of inhibitor A as

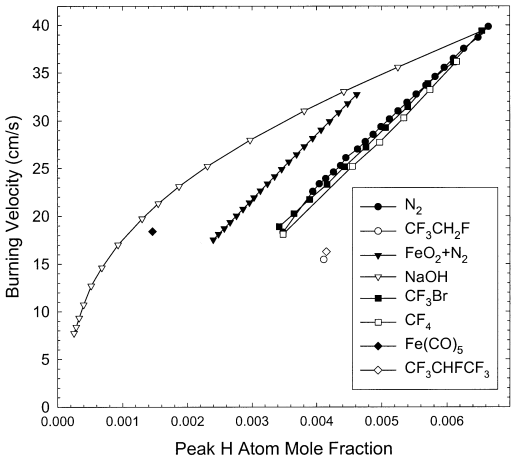

FIG 4. Relationship between burning velocity and peak concentration of atomic hydrogen for methane/air flames inhibited by various compounds. The N_2 + Fe data is that presented in Fig. 3, containing a FeO_2 as a reactant assumed to operate via an O + O inhibition cycle.

$$\Phi = \ln(U_A/U_{A+B})(X_{O2}/X_B) \quad (2)$$

where U_A and U_{A+B} are the burning velocities in the flames inhibited by inhibitor A alone and A and B in combination, respectively. The differential inhibition parameter of 500 ppm FeO_2 increases by some 23% as the flame temperature is lowered by nitrogen addition from 2230 to 2010 K. Saso et al. [4] found that the inhibition parameter of CF_3Br increased by some 45% (at both 0.5% and 1.0% mole fractions of agent) over the same range of final flame temperatures.

While the findings of synergism agree qualitatively between CF_3Br/inert and Fe/inert mixtures, the final flame temperature influences the inhibition parameter of CF_3Br twice as much as that of the O + O recombination cycle of iron, due to the lack of explicit temperature dependence of the Fe kinetic cycle. Thus, these results show that synergism in catalytic/inert mixtures does not require temperature dependence of the inhibition cycle, although this can influence its magnitude.

Correlation of Burning Velocities with Changes in Flame Structure

Padley and Sugden [19] observed in studies of $H_2/O_2/N_2$ flames that the burning velocity correlated with the partial pressure of atomic hydrogen in the reaction zone. More recently, this correlation has been observed to hold also for hydrogen flames inhibited by CF_3Br [20]. Fig. 4 plots the peak H atom concentration against burning velocity for a variety of inhibited methane/air flames. For methane flames inhibited by N_2, CF_4, and CF_3Br, there is a nearly identical linear relationship between the peak H-atom mole fraction and burning velocity, as with the hydrogen flames.

Examination of the effect of other inhibitors, however, demonstrates that this correlation is not a general one. The fluorocarbon agents CF_3CHFCF_3 and CF_3CH_2F both reduce burning velocity more than would be expected based on the peak H-atom concentrations. Inhibition by sodium or iron produces the opposite effect. Noteworthy in the sodium data is the curvature which coincides with the onset of saturation. The coincidence of the CF_3Br data points with those of the inert agents appears to be accidental. The calculations for the fluorocarbons and catalytic agents lie on opposite sides of those of the inert agents, and CF_3Br is in some sense a combination of the two.

An alternate correlation between burning velocity and flame structure can be based on the proportionality between the burning velocity and the square root of the overall reaction rate [4]. In modeling the burning velocity of a large number of inhibited flames, we find the burning velocity correlates in almost all cases with the product of the peak H-atom mole fraction and a global activation energy:

$$S_L^2 = A^2 X_H \exp(-E_a/kT_f) \quad (3)$$

where S_L is the laminar burning velocity, X_H the peak mole fraction of atomic hydrogen, and T_f the final flame temperature. The fitted parameters A and E_a, obtained by considering the flame inhibited by nitrogen, are A = 7940 cm/s, E_a = 24.7 kcal/mol. The same empirical correlation holds for inhibition by other inert gases, by iron and sodium, by nitrogen and iron in combination (Table 1), and by artificially increasing the H + OH recombination rate. For catalytic agents which do not significantly change the final flame temperature, the burning velocity correlates with the square root of the H-atom peak mole fraction, but not with those of atomic oxygen or OH radicals.

The effect of catalytic agents on reducing burning velocity appears to proceed through reduction of the atomic hydrogen concentration, whether or not the scavenging cycle directly involves H-atom recombination (as in the O + O cycle of iron). Table 1 compares the burning velocities estimated using equation 3 to the calculated values for a variety of flame inhibitors. In almost all cases, the reduction in burning velocity relative to the uninhibited flame predicted by equation 3 is within 10% of the result of the PREMIX calculation.

The correlation stated in equation 3 greatly underpredicts flame speed reduction by the fluorocarbons CHF_3 and C_3HF_7, as well as CF_3Br and HBr. Flame structure modeling indicates that the breakdown of this relationship involving the peak H-atom

TABLE 1
Comparison of calculated burning velocities to values from equation 3

$S_{eqn} = A(X_{H,max} \exp(-E_a/kT_{ad}))^{1/2}$ $A = 7940$ cm/s $E_a = 24.7$ kcal/mol

Flame Condition	$T_{adiabatic}$	$X_{H,max}$	S_{premix}	S_{eqn}	$\Delta S_{premix}/\Delta S_{eqn}$[a]
CH_4/air (uninhibited)	2234	6.64e − 3	39.8	39.8	—
+9.09% N_2	2121	5.12e − 3	30.2	30.2	1.00
+16.67% N_2	2015	3.94e − 3	22.6	22.7	1.01
+8.26% CF_4 (inert)	1968	3.50e − 3	18.4	19.9	1.07
+200 ppm $Fe(CO)_5$	2223	1.46e − 3	18.4	18.6	1.01
+1.0% CF_3Br	2203	3.42e − 3	18.9	27.6	1.71
+0.5% HBr	2221	5.36e − 3	30.3	35.2	2.08
+3.8% CF_3CH_2F	2031	4.11e − 3	15.5	23.9	1.54
+2.9% CF_3CHFCF_3	2161	3.86e − 3	16.3	26.1	1.73
+0.05% $(NaOH)_2$	2219	2.97e − 3	28.0	26.2	0.87
+0.40% $(NaOH)_2$	2177	3.31e − 4	9.4	8.3	0.97
Increase H + OH + M rate × 100	2234	1.35e − 3	19.8	18.0	0.92

[a] $(39.6 - S_{premix})/(39.6 - S_{eqn})$

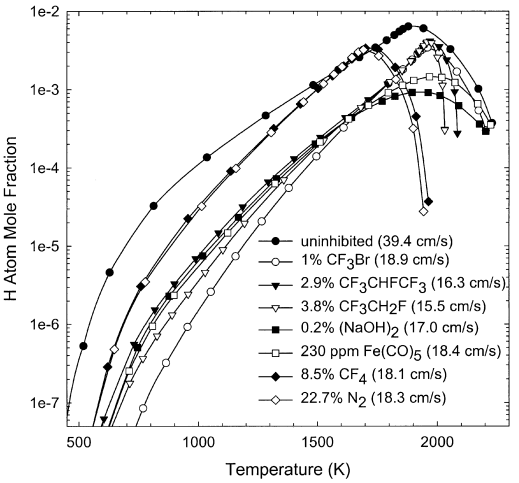

FIG 5. Mole fraction of atomic hydrogen as a function of local flame temperature for an uninhibited atmospheric pressure methane/air flame, and the same flame inhibited by the indicated suppression agents.

concentration is a consequence of these agents reducing the H-atom concentration mostly in the early part of the flame, prior to the peak concentration, as discussed below.

Changes in Flame Structure due to Different Agents

Insight into why the correlation between burning velocity, H-atom concentration, and temperature does not hold for either fluorocarbons or bromine-containing compounds can be gained from examination of these compounds' effects on flame structure. In Fig. 5, the mole fraction of atomic hydrogen is plotted against the local temperature for flames inhibited by a variety of agents. All the inhibited flames have burning velocities approximately 50% that of the uninhibited flame, whose structure is also plotted for comparison. For all the flames considered here, the temperature monotonically increases with position passing from reactants to products.

The relationship between H-atom mole fraction and local temperature shown in Fig. 5 appears to be characteristic of each type of agent except for CF_3Br. The physical agents reduce the final flame temperature, but the H-atom mole fraction at a given isotherm (above approximately 1300 K) is changed very little from its value in the uninhibited flame. Both iron and sodium reduce the H-atom mole fraction by a relatively constant factor throughout the reaction zone. The fluorocarbons reduce the H-atom mole fraction early in the flame (in the region below about 1200 K) but have relatively little impact on the peak concentration. This diminished effectiveness at the location of maximum hydrogen atom concentration also occurs for CF_3Br; in this respect, CF_3Br bears more resemblance to non-brominated fluorocarbons than it does to other catalytic agents such as iron and sodium. Since Babushok et al. [5] found that iron approaches the performance of an "ideal" catalytic inhibitor, the different effect of CF_3Br on flame structure from that of iron and sodium indicates a departure from ideality; in particular, it only scavenges radicals significantly in low-temperature regions of the flame. It is noteworthy that all the flames inhibited by chemically active suppressants

show nearly equal reductions in H-atom mole fraction at 1700 K. In the flames inhibited by inert agents, the H-atom concentration at this isotherm is essentially the same as in the uninhibited flame. Therefore, the H-atom mole fraction at 1700 K (or any other fixed temperature) cannot be used as a predictor of burning velocity which is applicable to all inhibited flames. Given the different influences of the suppressants on flame structure, it seems unlikely that an empirical relationship between flame speed and some other quantity can be found which applies to all suppressed flames.

The depletion of radical species early in the flame has a marked influence on the burning velocity. It is for this reason that fluorocarbons and bromine compounds are better inhibitors than the changes in temperature and peak H-atom concentrations would predict. This observation suggests that agents which deplete radicals in high-temperature regions but not early in the flame are likely to be less effective inhibitors than would otherwise be expected. This may be the case for condensed-phase agents which must vaporize before inhibition can begin.

Conclusions

We have modeled the effect of CF_3Br and other representative physical and chemical fire suppressants on the burning velocity and flame structure of premixed methane/air flames. In several respects, CF_3Br is not representative of catalytic fire suppressants in general. Several features of its kinetics, including the strong temperature dependence of the catalytic suppression cycle, the apparent absence of significant saturation effects for a burning velocity reduction of more than 50%, and the preferential reduction of atomic hydrogen concentrations in low-temperature regions of the flame, are not shared by other catalytic suppressants. Other catalytic agents including sodium and iron exhibit behavior much more typical of this class of suppressants. For these reasons, caution is required in extrapolating the suppression properties observed for CF_3Br to other fire suppressants.

Acknowledgments

We thank V. Babushok and G. Linteris for helpful discussions and for providing kinetic mechanisms used here. This work was supported by the Office of Naval Research through the Naval Research Laboratory and by the Department of Defense Next-Generation Fire Suppressant Technology Program, funded by the DoD Strategic Environmental Research and Development Program.

REFERENCES

1. Westbrook, C. K., *Combust. Sci. Technol.* 23:191–202 (1980).
2. Babushok, V., and Tsang, W., *Combust. Flame* 123:488–506 (2000).
3. Noto, T., Babushok, V., Hamins, A., and Tsang, W., *Combust. Flame* 112:147–160 (1998).
4. Saso, Y., Ogawa, Y., Saito, N., and Wang, H., *Combust. Flame* 118:489–499 (1999).
5. Babushok, V., Tsang, W., Linteris, G. T., and Reinelt, D., *Combust. Flame* 115:551–560 (1998).
6. Sheinson, R. S., Penner-Hahn, J. E., and Indritz, D., *Fire Safety J.* 15:437–450 (1989).
7. Zegers, E. J. P., Williams, B. A., Sheinson, R. S., and Fleming, J. W., *Proc. Combust. Inst.* 28:2931–2937 (2000).
8. McNesby, K. L., Daniel, R. G., Widder, J. M., and Miziolek, A. W., *Appl. Spectrosc.* 50:126–130 (1996).
9. Kee, R. J., Grcar, J. F., Smooke, M. D., and Miller, J. A., *PREMIX: A Fortran Program for Modeling Laminar One-Dimensional Premixed Flames,* Sandia report SAND85-8240.
10. Bowman, C. T., Hanson, R. K., Gardiner, W. C., Lissianski, V., Frenklach, M., Goldenberg, M., and Smith, G. P., *GRI-Mech 2.11—An Optimized Detailed Chemical Reaction Mechanism for Methane Combustion and NO Formation and Reburning,* GRI report GRI-97/0020, Gas Research Institute, Chicago, 1997, www.ME.Berkeley.edu/gri_mech.
11. L'Espérance, D., Williams, B. A., and Fleming, J. W., *Combust. Flame* 117:709–731 (1999).
12. Williams, B. A., L' Espérance, D. M., and Fleming, J. W., *Combust. Flame* 120:160–172 (2000).
13. Zamansky, V. M., Lissianski, V. V., Maly, P. M., Ho, L., Rusli, D., and Gardiner Jr., W. C., *Combust. Flame* 117:821–831 (1999).
14. Rumminger, M. D., and Linteris, G. T., *Combust. Flame* 120:451–464 (2000).
15. Rosser, W. A., Wise, H., and Miller, J., *Proc. Combust. Inst.* 7:175–182 (1958).
16. Rosser, W. A., Inami, S. H., and Wise, H., *Combust. Flame* 7:107–119 (1963).
17. Lott, J. L., Christian, S. D., Sliepcevich, C. M., and Tucker, E. E., *Fire Technol.* 32:260–271 (1996).
18. Linteris, G. T., Rumminger, M. D., Babushok, V., and Tsang, W., *Proc. Combust. Inst.* 28:2965–2972 (2000).
19. Padley, P. J., and Sugden, T. M., *Proc. Combust. Inst.* 7:235–242 (1958).
20. Kim, C. H., Kwon, O. C., and Faeth, G. M., "*Effects of Fire Suppressants on Hydrogen-fueled Premixed Flames,*" paper 219, U.S. Sections Second Joint Meeting of the Combustion Institute, Oakland, CA, CI March 25–28, 2001.